Projected-fields kSZ estimator

Ola Kusiak
University of Cambridge

14 October 2025, CMB France

Work with many people: Colin Hill, Boris Bolliet, Simone Ferraro, Raagini Patki, Nick Battaglia, Shivam Pandey, Michael Rodriguez+++

Projected-fields kSZ^2-LSS estimator

Main idea: foreground-cleaned blackbody CMB temperature map contains kSZ information

kSZ signal traces the overall mass distribution, and thus can be detected by cross-correlating it with any LSS field, e.g., galaxies, galaxy/CMB lensing

But <kSZ x LSS> vanishes! (electron velocity)

Solution: Square the kSZ field

Projected-field kSZ^2-LSS:

1. Construct a clean T map & apply Wiener filter
2. Square in real space
3. Cross-correlate with *projected* (2D) LSS tracer

No redshift estimates needed!

Doré et al. (2004); DeDeo et al. (2005); Hill et al.(2016), Ferraro et al. (2016), Kusiak et al. (2021), Bolliet et al. (2022), Patki et al. (2023)

What do we measure with projected-fields?

kSZ-induced temperature shift in the CMB:

$$\left[\Theta^{\mathrm{kSZ}}(\hat{\boldsymbol{n}}) = -\int_0^{\eta_{re}} d\eta\, g(\eta)\, \boldsymbol{p_e} \cdot \hat{\boldsymbol{n}} = -\sigma_T \int_0^{\eta_{re}} \frac{d\eta}{1+z} e^{-\tau} n_e(\hat{\boldsymbol{n}}, \eta) \boldsymbol{v_e} \cdot \hat{\boldsymbol{n}},\right]^2$$

Gas density profile

x

projected galaxy overdensity:

$$\delta_g(\hat{\boldsymbol{n}}) = \int_0^{\eta_{\max}} d\eta W_g(\eta) \delta_m(\eta\hat{\boldsymbol{n}}, \eta),$$

$W_g(\eta) = b_g(\eta) * p(\eta)$ - projection kernel

Redshift distribution

$$C_\ell^{\mathrm{kSZ}^2 \times \delta_g} = \frac{1}{c^2} \int_0^{\eta_{\max}} \frac{d\eta}{\eta^2} W_g(\eta) g^2(\eta) \mathcal{T}(k = \frac{\ell}{\eta}, \eta),$$

Triangle power spectrum:

$$\mathcal{T}(k, \eta) = \int \frac{d^2\boldsymbol{q}}{(2\pi^2)} f(q\eta) f(|\boldsymbol{k}+\boldsymbol{q}|\eta) \boxed{B_{\delta_g p_{\hat{n}} p_{\hat{n}}}(\boldsymbol{k}, \boldsymbol{q}, -\boldsymbol{k}-\boldsymbol{q}).}$$

'Hybrid' bispectrum

approx. as

$$B_{\delta_g p_{\hat{n}} p_{\hat{n}}} = \frac{1}{3} v_{\mathrm{rms}}^2 B_{\mathrm{m}}^{\mathrm{NL}} .$$

Doré et al. (2004); DeDeo et al. (2005); Hill et al.(2016), Ferraro et al. (2016), Kusiak et al. (2021), Bolliet et al. (2022), Patki et al. (2023)

What can we learn from the projected-fields kSZ?

$$C_\ell^{\mathrm{kSZ}^2 \times \delta_g} \propto f_b^2 f_{\mathrm{free}}^2 \times \frac{1}{3} v_{\mathrm{rms}}^2 \times \text{(galaxy bias, etc)}$$

baryon fraction

free electron fraction

large-scale velocity dispersion

Large scale limit: <u>baryon abundance can be constrained</u>

Halo model: <u>shape of gas density profile</u>

Upcoming CMB experiments!

Caution!! squaring a lensed filtered T map reconstructs the lensing potential:

$\langle T_{\mathrm{CMB}}^2 \times g \rangle \propto C^{\Psi g}$ → **projected-fields has a CMB lensing contribution**

Doré et al. (2004); DeDeo et al. (2005); Hill et al.(2016), Ferraro et al. (2016), Kusiak et al. (2021), Bolliet et al. (2022), Patki et al. (2023)

Projected-fields kSZ with *unWISE* and *Planck*

CMB:

- LGMCA blackbody temperature map (tSZ-deprojected), based on *Planck* and *WMAP*
- *Planck* SMICA maps

Number density of galaxies

unWISE	$\bar{z}$	δ_z	$\bar{n}$
blue	0.6	0.3	3409
green	1.1	0.4	1846
red	1.5	0.4	144

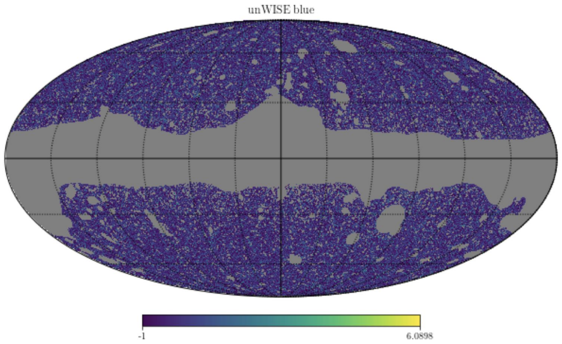

***unWISE* catalog** (Krolewski et al. 2021):

- Based on WISE and NEOWISE
- Over 500 million galaxies on the full sky
- 3 subsamples: blue (z=0.6), green (z=1.1), and red (z=1.5)

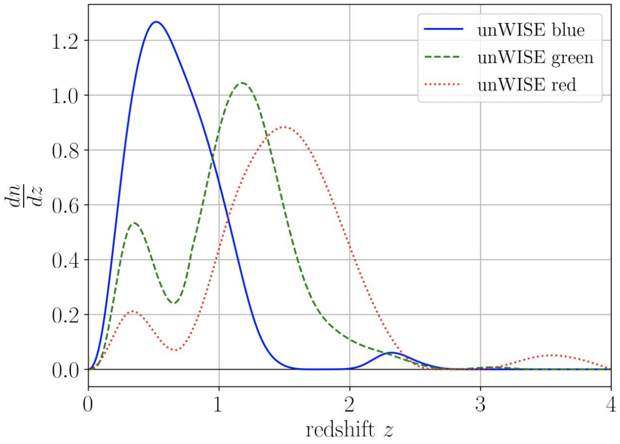

Krolewski et al. 2021, Kusiak et al. 2021

kSZ with *unWISE* and *Planck*: Results

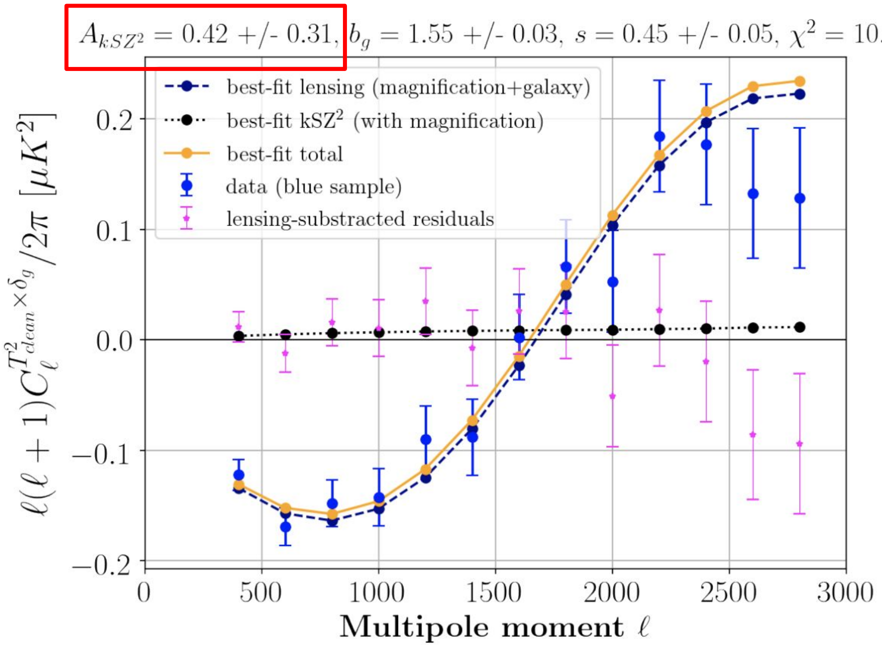

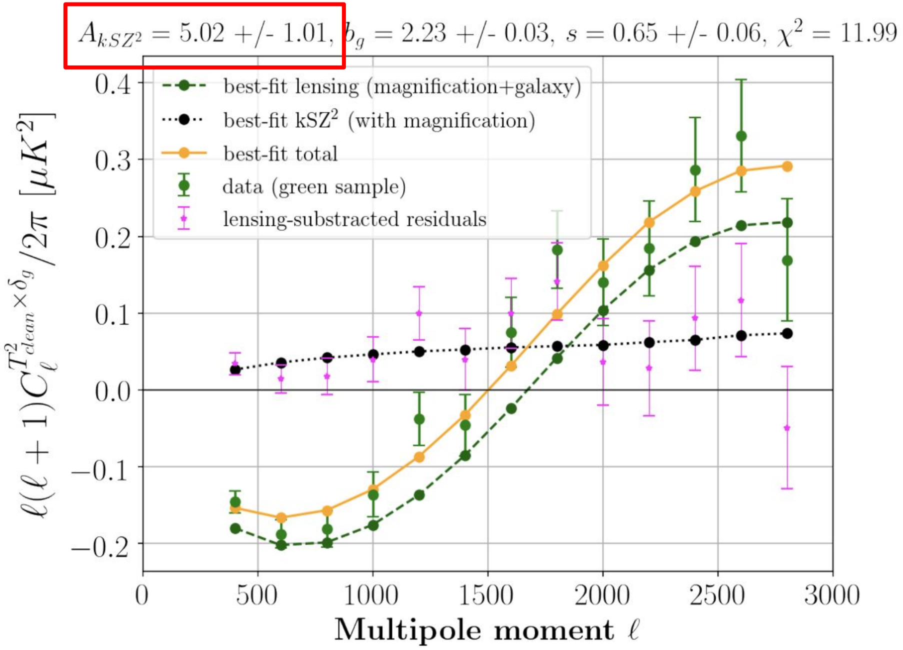

Blue (z~0.6): $(f_b/0.158)\,(f_{free}/1.0) = 0.65$ +/- 0.24

Green (z~1.1): $(f_b/0.158)\,(f_{free}/1.0) = 2.24$ +/- 0.23

Red (z~1.5): $(f_b/0.158)\,(f_{free}/1.0) = 2.87$ +/- 0.56

+Red (highest redshift kSZ detection)

Overall S/N ~5.5

No missing baryons!

Kusiak et al. 2021

Halo-model kSZ^2 x LSS

$$\boxed{C_\ell^{\mathrm{kSZ}^2 X} = \int \mathrm{d}v W^{\mathrm{kSZ}}(\chi)^2 W^X(\chi) T(\ell,\chi) \quad \text{with} \quad T(\ell,\chi) = \int \frac{\mathrm{d}^2\boldsymbol{\ell}'}{(2\pi)^2} w(\ell') w(|\boldsymbol{\ell}+\boldsymbol{\ell}'|) B_{\delta_e\delta_e X}(\mathbf{k}_1,\mathbf{k}_2,\mathbf{k}_3)}$$

- Halo model hybrid bispectrum

$$B_{\delta_e\delta_e X} = B^{1h}_{\delta_e\delta_e X} + B^{2h}_{\delta_e\delta_e X} + B^{3h}_{\delta_e\delta_e X}$$

X - LSS tracer

$$B^{1h}_{\delta_e\delta_e X} = \int \mathrm{d}n_1 \hat{u}^{e}_{k_1}(m_1)\hat{u}^{e}_{k_2}(m_1)\hat{u}^{X}_{k_3}(m_1)$$

1 halo

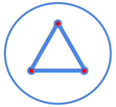

$$B^{2h}_{\delta_e\delta_e X} = \int \mathrm{d}n_1 b^{(1)}(m_1)\hat{u}^{e}_{k_1}(m_1)\hat{u}^{e}_{k_2}(m_1) \int \mathrm{d}n_2 b^{(1)}(m_2)\hat{u}^{X}_{k_3}(m_2) P_L(k_3) + \text{perms}$$

2 halo

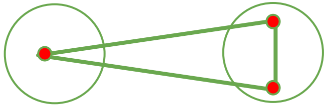

$$B^{3h}_{\delta_e\delta_e X} = 2\int \mathrm{d}n_1 b^{(1)}(m_1)\hat{u}^{e}_{k_1}(m_1)P_L(k_1) \int \mathrm{d}n_2 b^{(1)}(m_2)\hat{u}^{e}_{k_2}(m_2)P_L(k_2) \int \mathrm{d}n_3 b^{(1)}(m_3)\hat{u}^{X}_{k_3}(m_3) F_2(k_1,k_2,k_3)$$
$$+ \int \mathrm{d}n_1 b^{(1)}(m_1)\hat{u}^{e}_{k_1}(m_1)P_L(k_1) \int \mathrm{d}n_2 b^{(1)}(m_2)\hat{u}^{e}_{k_2}(m_2)P_L(k_2) \int \mathrm{d}n_3 b^{(2)}(m_3)\hat{u}^{X}_{k_3}(m_3) + \text{perms}$$

Liner matter power spectrum

Fourier transform of the gas density profile/tracer

3 halo

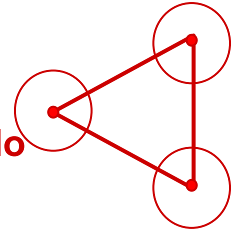

Implemented in halo-model code [class-sz]

Bolliet,..., AK,… 2022; Bolliet, AK, et al. 2023, Bolliet, AK, et al. 2025

Halo-model kSZ^2 x LSS

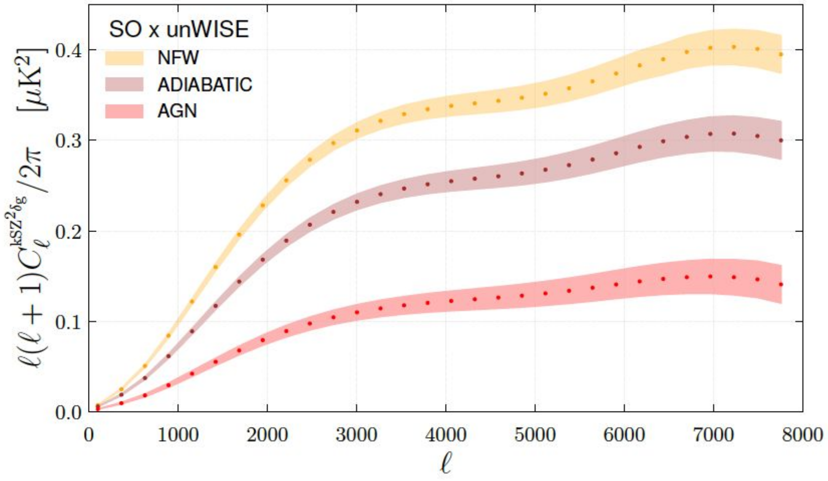

		SNR$_{\mathrm{tot}}$	$(\frac{\Delta A_0^\beta}{A_0^\beta})^{-1}$	$(\frac{\Delta A_0^\alpha}{A_0^\alpha})^{-1}$	$(\frac{\Delta f_{\mathrm{free}}}{f_{\mathrm{free}}})^{-1}$
δ_g	*Planck* × *unWISE*	1.7	0.18 (0.37)	0.29 (0.38)	0.19 (10)
	AdvACT × *unWISE*	17.8	1.72 (2.87)	2.22 (2.54)	0.71 (10)
	SO × *unWISE*	61.9	3.70 (5.51)	2.07 (4.98)	0.78 (10)
	CMB-S4 × *unWISE*	102.9	7.32 (7.83)	2.38 (7.18)	1.12 (10)
κ_g	AdvACT × DES	2.24	0.28 (0.79)	0.59 (0.88)	0.09 (10)
	AdvACT × VRO/*Euclid*	5.98	0.92 (2.11)	1.72 (2.44)	0.31 (10)
	SO × DES	6.14	1.03 (2.75)	0.93 (2.34)	0.23 (10)
	SO × VRO/*Euclid*	18.81	3.89 (6.84)	3.24 (8.22)	0.88 (10)
	CMB-S4 × DES	9.71	2.19 (4.36)	1.33 (5.23)	0.40 (10)
	CMB-S4 × VRO/*Euclid*	29.72	8.57 (13.07)	4.71 (15.08)	1.51 (10)
κ_{cmb}	SO	16.39	0.92 (2.84)	1.72 (2.72)	0.94 (10)
	CMB-S4	34.52	2.76 (7.01)	5.75 (7.79)	2.4 (10)

Fisher forecasts for constraints on baryon profile→ with SO and LSS tracers: Galaxy density **(60σ)**, Galaxy lensing **(18σ)**, CMB lensing **(16σ)**

Bolliet,..., AK,... 2022

Improved Modeling of Projected-fields kSZ

Raagini Patki, Cornell

Improved theoretical model for $B_{p_n p_n \delta}$ derived in Patki et al. (2023)

Considers *all terms in* $B_{p\,p\,\delta}$ (not just the the dominant v^2 * B) & valid for *all (esp. squeezed) triangle shapes*

- => **Significant** scale-dependent **differences** in predicted theoretical signal: 10-15%
- To be incorporated into class_sz pipeline
- Cosmological dependence characterized

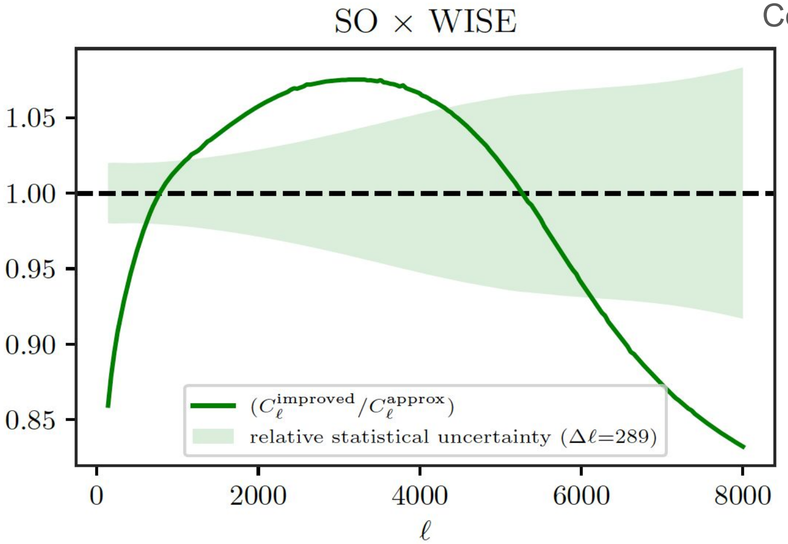

Ratio of the improved / approximated models compared with the SO errorbars on kSZ^2

Patki et al. 2023

Comparison of halo-model with simulations

Michael Rodriguez
Columbia Bridge student

Comparison of the halo-model implementation (class_sz) with sims (Websky) inspired by the Patki et al. 2023 results:

- Validated on tSZ and tau maps
- Cross-correlation with halos at different mass and redshift bins

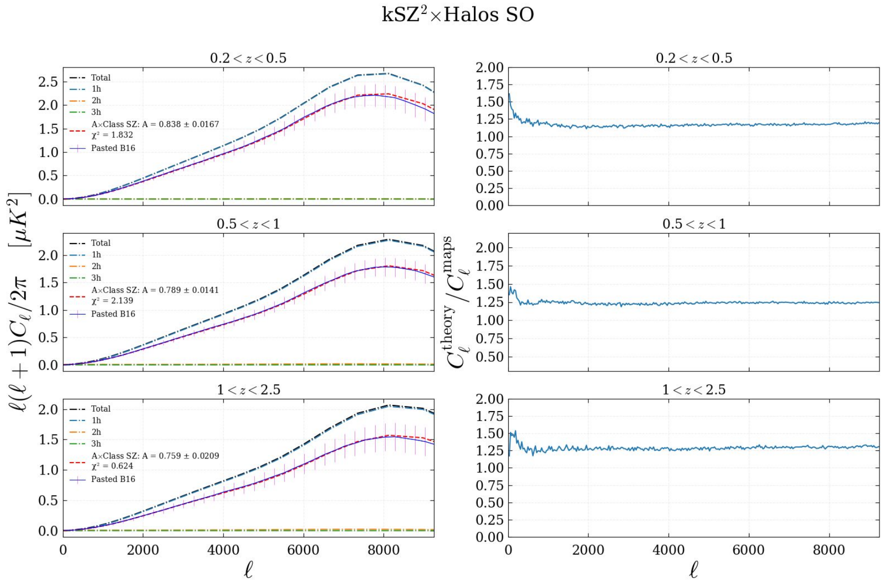

Ratio halo-model class_sz / Websky sims for the Battaglia16 profile shows very little angular dependency

2509.03458

Rodriguez et al. 2025

Remove the lensing: bias-hardened kSZ

1. **Lensing term in kSZ2**: squaring a **lensed** T map reconstructs the lensing potential: $\langle T_{CMB}^2 \times g \rangle \propto C^{\Psi g}$ → **projected-fields = non optimal lens estimator**
    - So far marginalized over
2. **Bias-hardening** :
    - Originally for lensing reconstruction (Namikawa et al. 2012)
    - Aims to isolate the lensing potential from **other sources of mode-coupling** present in the reconstruction, e.g., tSZ or Poisson-distributed point sources
    - Routinely used for QE reconstruction, e.g., tSZ-hardening of lensing (Qu et al. 2023)

Do the opposite: lensing-harden the kSZ^2 estimator

Kusiak et al. in prep.

Remove the lensing: bias-hardened kSZ

Tested on AGORA sims (Omori 2022)--works pretty well! (bias-hardened close to the true kSZ signal)

Bahamas 76–low feedback

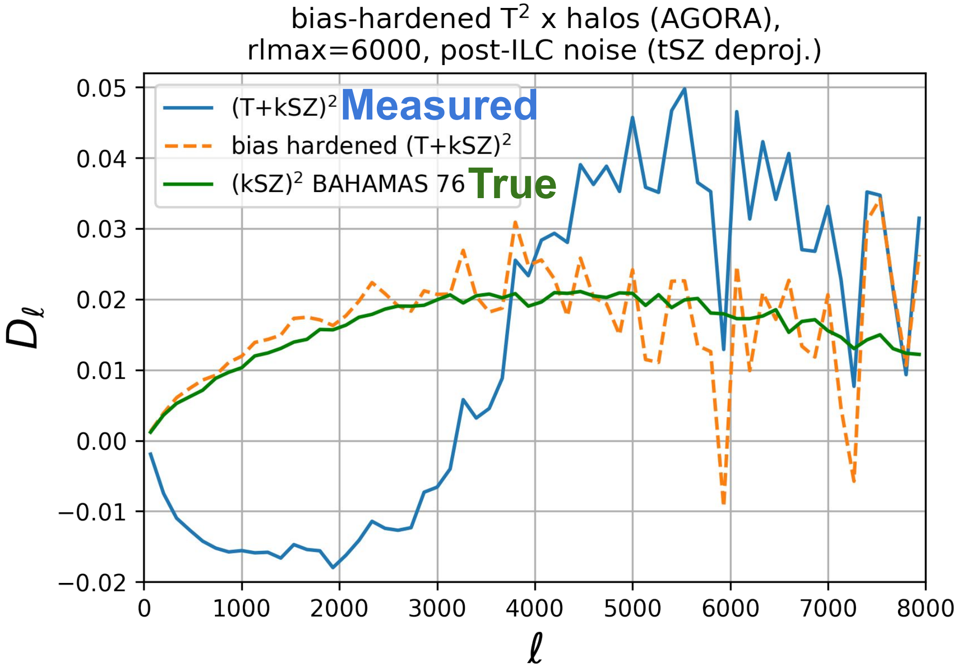

Bahamas 80–large feedback

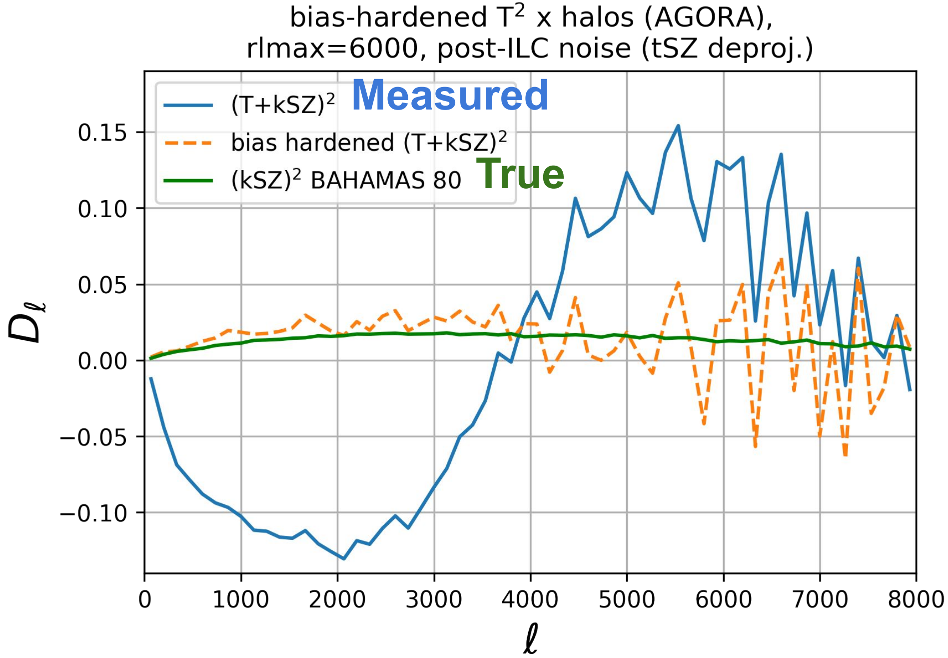

Kusiak et al. in prep.

Projected-fields kSZ with *unWISE* and ACT DR6

with *Planck*

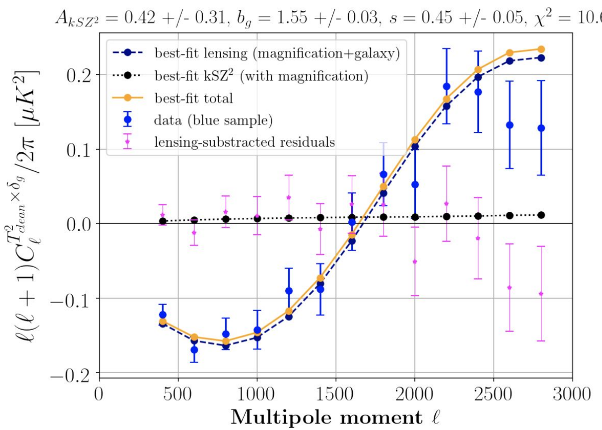

with ACT DR6

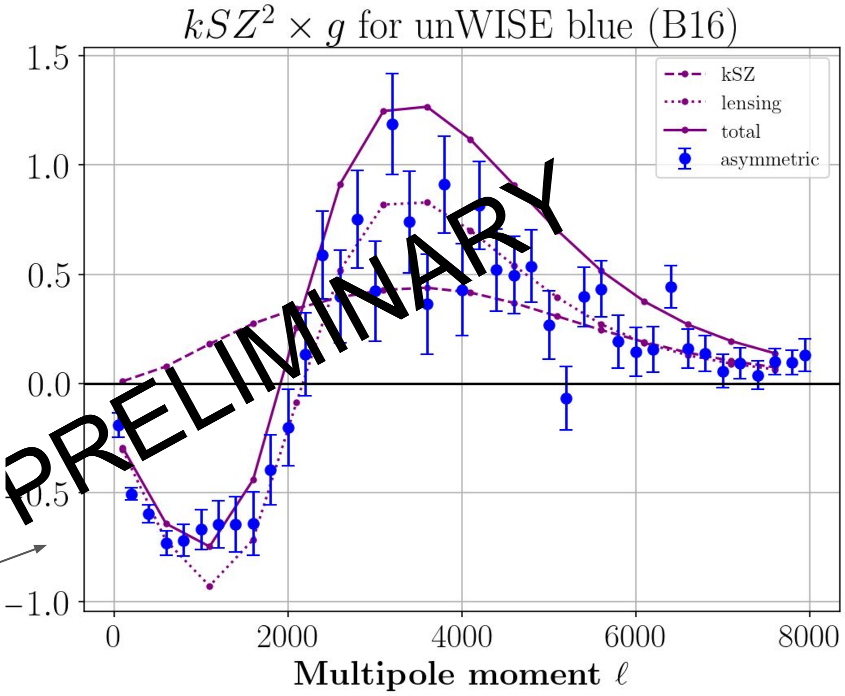

Measurement is again lensing dominated

Theory curve is not a fit! (only used *unWISE* HOD, and B16 AGN gas density profile)

Goal: constrain *unWISE* **density profile**

Analysis in progress!

Kusiak et al. in prep.

Summary

1. Projected-field kSZ – squaring the temperature map to avoid cancellation of the signal
    a. No need for spectroscopic redshifts
2. Lots of cool developments recently:
    - Improved modeling and bispectrum estimator (Patki et al.)
    - Comparison with sims (Rodriguez et al.)
    - Bias-hardening to remove the lensing contribution
3. Measurement with DR6 ongoing and exciting prospects for SO!

What do we measure with projected-fields?

‘Hybrid’ bispectrum

$$\mathcal{T}(k,\eta) = \int \frac{d^2\boldsymbol{q}}{(2\pi^2)} f(q\eta) f(|\boldsymbol{k}+\boldsymbol{q}|\eta) \boxed{B_{\delta_g p_{\hat{\boldsymbol{n}}} p_{\hat{\boldsymbol{n}}}}(\boldsymbol{k},\boldsymbol{q},-\boldsymbol{k}-\boldsymbol{q}).}$$

Projected-fields squeezes the rich information from the bispectrum into a power spectrum estimator

Hybrid bispectrum <kSZ kSZ g> modeling:

1. Originally the dominant contraction only, approx. as velocity dispersion x non-linear matter bispectrum (in Hill 2016, Ferraro 2016, Kusiak 2021)

$$B_{\delta_g p_{\hat{\boldsymbol{n}}} p_{\hat{\boldsymbol{n}}}} \approx \frac{1}{3} v_{\mathrm{rms}}^2 B_{\mathrm{m}}^{\mathrm{NL}}$$

2. **Bolliet et al.** still the dominant contraction only, but in the **halo model** (Bolliet et al. class_sz)
3. **Patki et al.** considers *all terms* to the hybrid bispectrum

Doré et al. (2004); DeDeo et al. (2005); Hill et al.(2016), Ferraro et al. (2016), Kusiak et al. (2021), Bolliet et al. (2022), Patki et al. (2023)

kSZ with *unWISE* and *Planck*: Foreground

Foregrounds:

- **deproject tSZ:** asymmetric method
  - One leg is a tSZ-deprojected blackbody T map
- **CIB:** cleaning using the fact that <kSZ x g>=0
  - Construct T_clean:

$$T_{\mathrm{clean}} = (1+\alpha_{\mathrm{min}})T - \alpha_{\mathrm{min}} T_{\mathrm{dust}}\,,$$

such that **$\langle T_{\mathrm{clean}}$ x g $\rangle = 0$**

CIB tracer = *Planck* 545/857 GHz

Null tests:

T_clean**Planck* 545 x g

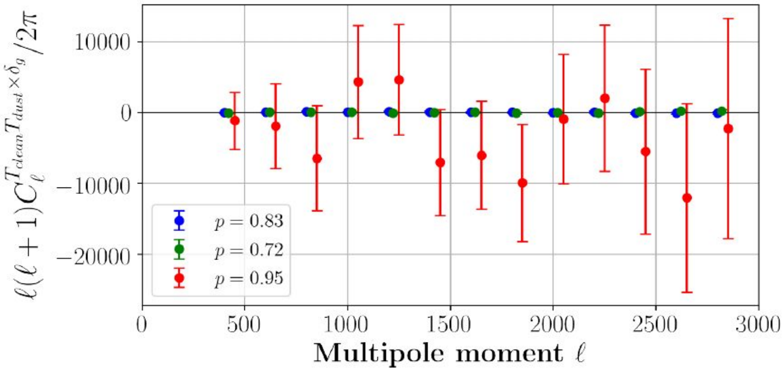

\+ w/ *Planck* 857 GHz
\+ T_{noise} / T^2_{noise} tests
\+ Additional assessment of the CIB level

All consistent with null

Kusiak et al. 2021

kSZ with *unWISE* and ACT DR6: Null tests

<T_clean x g> test

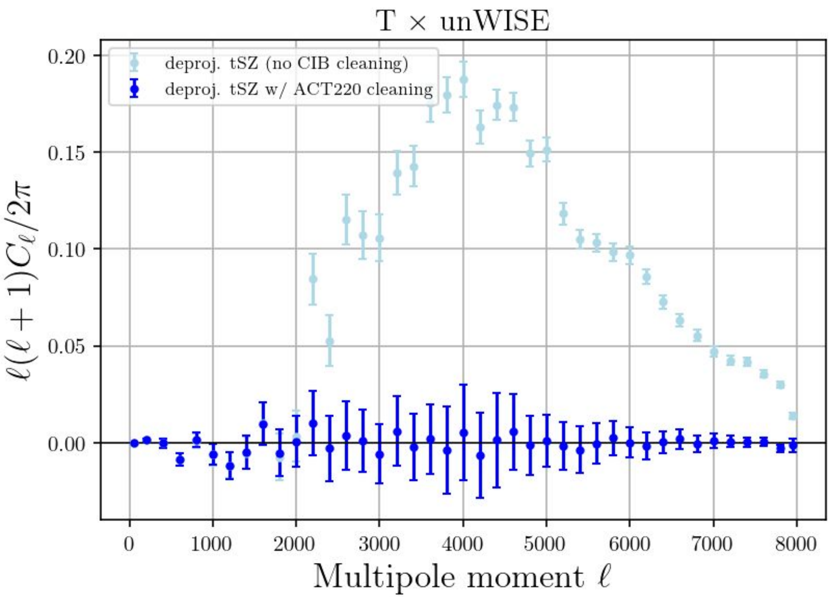

<T x g> is expected to be zero if T is truly blackbody (kSZ+CMB)

<T_dustT_clean x g> test

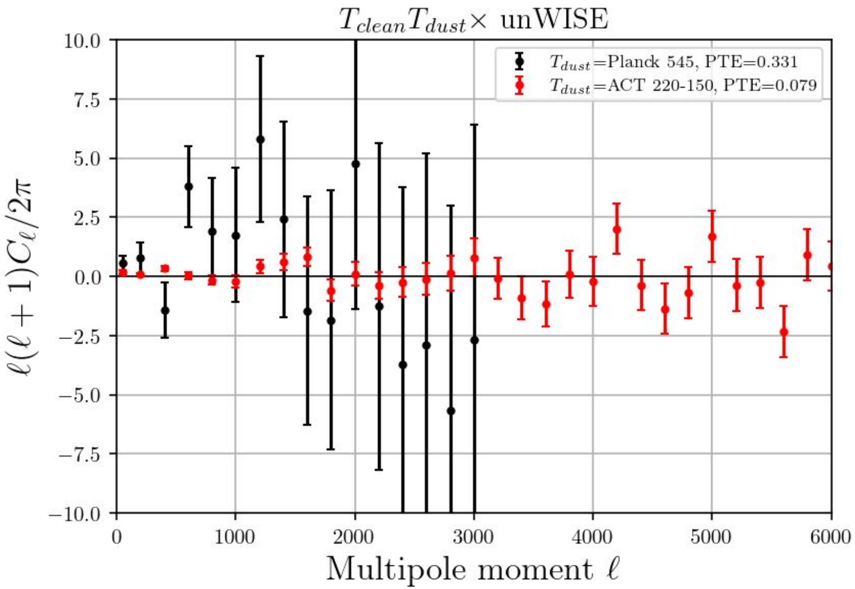

very powerful test–it will pick up any residual CIB/tSZ contamination in T_clean

Projected-fields kSZ: Lensing contribution

Lensed CMB fluctuations: $\tilde{\Theta}(\mathbf{x}) = \Theta(\mathbf{x}) + \nabla\psi \cdot \nabla\Theta(\mathbf{x}) + \ldots$

Up to first order in the lensing potential we have

$$\langle \tilde{\Theta}(\mathbf{L})\tilde{\Theta}(\boldsymbol{\ell}_1 - \mathbf{L})\delta_g(\boldsymbol{\ell}_2)\rangle = \langle \Theta(\mathbf{L})\Theta(\boldsymbol{\ell}_1 - \mathbf{L})\delta_g(\boldsymbol{\ell}_2)\rangle +$$
$$\boxed{\langle [\nabla\psi \cdot \nabla\Theta](\mathbf{L})\tilde{\Theta}(\boldsymbol{\ell}_1 - \mathbf{L})\delta_g(\boldsymbol{\ell}_2)\rangle + (\mathbf{L} \to \boldsymbol{\ell}_1 - \mathbf{L}) +} \ldots$$

$$\Downarrow$$

$$-2\int \frac{d^2\mathbf{L}}{(2\pi)^2} f(L) f(|\boldsymbol{\ell}_1 - \mathbf{L}|) \int \frac{d^2\mathbf{L}'}{(2\pi)^2} \mathbf{L}' \cdot (\mathbf{L} - \mathbf{L}') \boxed{\langle \psi(\mathbf{L}')\Theta(\mathbf{L} - \mathbf{L}')\Theta(\boldsymbol{\ell}_1 - \mathbf{L})\delta_g(\boldsymbol{\ell}_2)\rangle} + \ldots$$

$$\boxed{\langle \psi\delta_g\rangle\langle\Theta\Theta\rangle} \qquad \cancel{\langle\psi\Theta\rangle\langle\Theta\delta_g\rangle}$$

$$\Downarrow$$

Leading order lensing contribution:

$$\Delta C_\ell^{T^2\times\delta_g} \approx -2\frac{\ell\, \boxed{C_\ell^{\psi\delta_g}}}{(2\pi)^2} \int_0^\infty dL'\, L'^2 f(L') \boxed{C_{L'}^{TT}} \int_0^{2\pi} d\phi\, f(|\mathbf{L}' + \boldsymbol{\ell}|) \cos\phi$$

Ferraro et al. 2016